



Published in final edited form as:

Acc Chem Res. 2017 September 19; 50(9): 2297–2308. doi:10.1021/acs.accounts.7b00265.

Bioorthogonal Cycloadditions: Computational Analysis with the Distortion/Interaction Model and Predictions of Reactivities

Fang Liu^{†,‡,iD}, Yong Liang^{*,†}, and K. N. Houk^{*,‡,iD}

[†]State Key Laboratory of Coordination Chemistry, School of Chemistry and Chemical Engineering, Nanjing University, Nanjing 210023, China

[‡]Department of Chemistry and Biochemistry, University of California, Los Angeles, California 90095, United States

CONSPECTUS

Bioorthogonal chemistry has had a major impact on the study of biological processes in vivo. Biomolecules of interest can be tracked by using probes and reporters that do not react with cellular components and do not interfere with metabolic processes in living cells. Much time and effort has been devoted to the screening of potential bioorthogonal reagents experimentally. This Account describes how our groups have performed computational screening of reactivity and mutual orthogonality. Our collaborations with experimentalists have led to the development of new and useful reactions. Dozens of bioorthogonal cycloadditions have been reported in the literature in the past few years, but as interest in tracking multiple targets arises, our computational screening has gained importance for the discovery of new mutually orthogonal bioorthogonal cycloaddition pairs. The reactivities of strained alkenes and alkynes with common 1,3-dipoles such as azides, along with mesoionic sydnone and other novel 1,3-dipoles, have been explored. Studies of “inverse-electron-demand” dienes such as triazines and tetrazines that have been used in bioorthogonal Diels–Alder cycloadditions are described. The color graphics we have developed give a snapshot of whether reactions are fast enough for cellular applications (green), adequately reactive for labeling (yellow), or only useful for synthesis or do not occur at all (red). The colors of each box give an instant view of rates, while bar graphs provide an analysis of the factors that control reactivity. This analysis uses the distortion/interaction or activation strain model of cycloaddition reactivity developed independently by our group and that of F. Matthias Bickelhaupt in The Netherlands. The model analyzes activation barriers in terms of the energy required to distort the reactants to the transition state geometry. This energy, called the distortion energy or activation strain, constitutes the major component of the activation energy. The strong bonding interaction between the termini of the two reactants, which we call the interaction energy, overcomes the distortion energy and leads to the new bonds in the products. This Account describes how we have analyzed and predicted bioorthogonal cycloaddition reactivity using the distortion/interaction model and how our experimental collaborators have employed these insights

*Corresponding Authors, houk@chem.ucla.edu, yongliang@nju.edu.cn.

ORCID

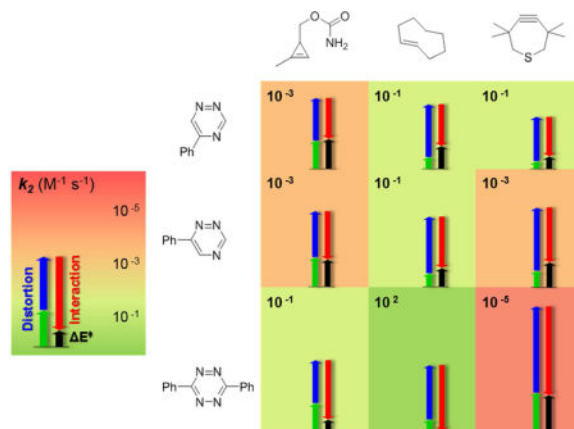
Fang Liu: 0000-0002-0046-8434

K. N. Houk: 0000-0002-8387-5261

The authors declare no competing financial interest.

to create new bioorthogonal cycloadditions. The graphics we use document and predict which combinations of cycloadditions will be useful in bioorthogonal chemistry and which pairs of reactions are mutually orthogonal. For example, the fast reaction of 5-phenyl-1,2,4-triazine and a thiacycloheptyne will not interfere with the other fast reaction of 3,6-diphenyl-1,2,4,5-tetrazine and a cyclopropene. No cross reactions will occur, as these are very slow reactions.

Graphical Abstract



I. INTRODUCTION

In the long history of organic synthesis, cycloaddition reactions are among the most powerful tools to obtain carbocycles and heterocycles, which are often components of natural products and pharmaceuticals.¹ The 1,3-dipolar cycloaddition² and the Diels–Alder reaction³ are the most commonly used cycloadditions to form five-membered heterocycles and six-membered carbocycles or heterocycles. Much effort has been devoted to investigating the reactivities and selectivities of these reactions, both experimentally and computationally. Our group has studied a variety of cycloaddition reactions in detail, including their mechanisms, intrinsic reactivities affected by electronic and steric factors, and regio- and stereochemistries.⁴ In the course of our systematic studies of cycloadditions, we developed a theoretical model (the distortion/interaction (D/I) model⁵ or activation strain model⁶) to understand quantitatively the origins of reactivities and selectivities. With the D/I model, we successfully explained the relative reactivities of a series of 1,3-dipoles,^{5a} the tendencies for cycloaddition reactivities of cyclic alkenes as dienophiles or dipolarophiles to increase dramatically as the ring size decreases,⁷ and the mutual orthogonality of different bioorthogonal cycloadditions.⁸ This orthogonal reactivity has recently gained much attention for applications in live-cell imaging. We describe how the D/I model has provided understanding and a useful guide to the development of bioorthogonal cycloadditions.

The concept of bioorthogonal reactions was first defined by Bertozzi in 2003.⁹ It refers to reactions that can occur in living systems without interfering with native biological processes. Figure 1 represents the bioorthogonal cycloaddition between a reporter that has been attached to a target biomolecule (here a protein) by a covalent or non-covalent link and a probe molecule that has a fluorescent group (symbolized by the red star) installed for the

purpose of imaging. The rapid cycloaddition between the probe and the reporter enables labeling of the target molecule and subsequent imaging to locate the target in the living cell. The probe and reporter are both bioorthogonal reagents that are inert to cellular components such as water, thiols, and amines but highly reactive with each other.

For in vivo applications, the rate constants of the cycloaddition reactions should be $1 \text{ M}^{-1} \text{ s}^{-1}$ or higher. This requirement arises from the low concentration of specific proteins or other biomolecules in the cellular environment.¹⁰ Figure 2 shows examples of known bioorthogonal processes and the range of rate constants that are useful for various potential applications. The examples are color-coded according to their rate constants. These examples are (1) Bertozzi's Staudinger ligation,¹¹ one of the first bioorthogonal reactions, but not a cycloaddition; (2) Bertozzi's "Cu-free click chemistry" with a strained cyclooctyne;¹² (3) the Sharpless click reaction,¹³ a Cu-catalyzed azide-alkyne reaction; and (4) a tetrazine ligation with a *trans*-cyclooctene.¹⁴ Green (1 to $10^5 \text{ M}^{-1} \text{ s}^{-1}$) indicates that the reaction is good for in vivo bioorthogonal chemistry to follow metabolic processes, and yellow (10^{-3} to $1 \text{ M}^{-1} \text{ s}^{-1}$) indicates reactions suitable for labeling but not to track metabolism, while red ($<10^{-3} \text{ M}^{-1} \text{ s}^{-1}$) shows that the reaction is too slow to be used in bioorthogonal chemistry. Such reactions may still be useful for synthetic purposes, where high concentrations and temperatures may be employed.

The commonly used probes and reporters meet the bioorthogonality requirements to various degrees. Some are extremely stable in biological environments, such as azides and unstrained alkynes. Others, like tetrazines, degrade by water or thiol additions that are, however, slow compared with the cycloaddition reactions. Besides the necessity of being orthogonal to cellular components, mutual orthogonality between the bioorthogonal reactants is another useful property.

Figure 3 shows an example of two bioorthogonal cycloaddition pairs that are also mutually orthogonal. *trans*-Cyclooctene reacts with tetrazines at a much higher rate than with azides, while dibenzoazacyclooctyne, a sterically hindered cyclooctyne, reacts with azides but not tetrazines. The D/I model explains the observed mutual orthogonality and has predicted other orthogonal reaction pairs that were later confirmed by our collaborators (as discussed later).

II. DISTORTION/INTERACTION (D/I), ACTIVATION STRAIN (AS), AND OTHER REACTIVITY MODELS

The D/I or AS model is a relatively new tool for chemists to understand reactivities and selectivities, but it actually has its origins in the work of Keiji Morokuma in the 1970s.¹⁵ Morokuma was developing an energy decomposition analysis to apply to molecular complexes and reactivities and noted that when molecules interact, they distort from their equilibrium geometries. He called the energy required to distort the molecules into the new geometries the "deformation energy".¹⁵ Later in that decade, Houk and co-workers analyzed the relative reactivities of alkynes and alkenes and described this quantity as the distortion energy.¹⁶ Recently, we developed a more general model, the distortion/interaction model.⁵ Bickelhaupt also developed such a model and called this distortion energy by a different

term, activation strain,⁶ to signify strain that is introduced into reactants as they achieve the transition state geometry. This model is the most recent in a long history of reactivity models, including the Evans–Polanyi treatment and its qualitative version, the Hammond–Leffler postulate, Morokuma’s energy decomposition analysis, Fukui’s frontier molecular orbital theory, Marcus theory, and the Woodward–Hoffmann rules.

The D/I model has been applied to a broad range of reactions, including organometallic reactions and nucleophilic additions as well as cycloaddition reactions. Several reviews of the D/I model in the literature describe the model in detail and its applications to all types of reactions.^{6,17} This Account focuses on the applications of the D/I model to bioorthogonal cycloadditions.

One dramatic example of the power of the D/I model is our study of different reactivities of cycloalkenes or cycloalkenones that have different ring sizes.⁷ In both cases, the three- and four-membered-ring dienophiles show unusually high reactivity in reactions with cyclopentadiene. One may argue that this is simply a result of strain release, but a closer look at the reaction with the D/I model shows that it is the difference in distortion energies in the transition states that leads to the high cycloaddition reactivities of small-ring compounds. The out-of-plane bending, which is the primary distortion of cycloalkenes or cycloalkenones in cycloaddition reactions, is less energy-consuming in three- and four-membered rings because of the higher s character in the hybridization states of the olefin. Recent analyses by Brian Levandowski and the Bickelhaupt group have shown that the position of the transition states is changed by the differences in interaction energies as well, causing very early undistorted transition states with cyclopropene and much later, more distorted transition states with cyclohexene.^{7c}

Figure 4 illustrates a D/I analysis using the reaction between cyclopentadiene and ethylene as an example. The solid black curve represents the potential energy surface along the reaction coordinate, starting from separate reactants at the left, through the transition state in the middle, and then to the cyclic adduct at the right. The black arrow represents the activation barrier for this specific reaction. The transition structure is separated into two fragments—here cyclopentadiene and ethylene distorted into the transition structure geometries. The energy difference between the distorted structures and their equilibrium geometries is termed the distortion energy (the blue arrow and green arrow). The red arrow represents the stabilizing interaction between the two pieces. The sum of the distortion energy and the interaction energy is the activation energy of the reaction.

III. APPLICATIONS TO BIOORTHOGONAL CYCLOADDITION

Our density functional theory (DFT) calculations were performed with Gaussian 09.¹⁸ Geometry optimizations were carried out at the M06-2X¹⁹ level of theory with the 6-31G(d) basis set. Solvent effects in water were evaluated at the M06-2X/6-311+G(d,p) level with a self-consistent reaction field (SCRF) using the CPCM model²⁰ on the gas-phase-optimized structures. Experimentally measured second-order rate constants k_2 for several well-studied bioorthogonal cycloadditions (shown in Figure 5) were used to calibrate our computational method.

Figure 6 shows the correlation between the calculated activation free energies and the experimentally measured values (derived from k_2 via the Eyring equation). Our computations tend to overestimate the reaction barriers more in relatively slow reactions than in rapid ones. With a systematic correction to the computed activation free energies, we can reproduce the observed kinetics within acceptable accuracy.

1. Cyclooctynes and Analogues with Azides

Since strain-promoted 1,3-dipolar cycloadditions of azides were introduced into bioorthogonal chemistry, great efforts have been made to develop new bioorthogonal reagents that react rapidly and selectively without interrupting native biological processes. A series of cyclooctynes, benzocyclooctadienyne, and aza analogues were reported (Figure 7a),^{12,22} among which biarylazacyclooctynone (BARAC) reacts most rapidly with azides. We studied the increase in reactivity in cyclooctynes compared with unstrained acetylene,^{23a} which was our first application of the D/I model to bioorthogonal chemistry. We collaborated with the Bertozzi group to understand the effects of strain and electronics on reactivities (Figure 7).^{23b}

Figure 8 shows the D/I diagrams for compound **1** (representative of the monosubstituted analogues **2–7**) and three other analogues (**8–10**) that show very different reactivities. The electronic effect introduced by a fluoride or methoxy group on the aryl rings is not significant, since the calculated activation energies for these compounds (**2–7**) are very close to that for **1**. Difluoro-BARAC (**8**) exhibits a stronger interaction energy and therefore a lower activation barrier, while the peri substituents on **9** and **10** introduce steric effects that increase the distortion energy and result in higher activation barriers.

2. Mutual Orthogonality in Bioorthogonal Cycloadditions

Encouraged by the success of the D/I model in explaining the reactivities of BARAC analogues with azide in bioorthogonal cycloadditions, we extended our analysis to cycloadditions of *trans*-cyclooctene with tetrazines and the orthogonal cycloadditions of dibenzocyclooctynes with azides. Various strain-promoted (3 + 2) cycloadditions reactions were developed, and high rate constants ($>1 \text{ M}^{-1} \text{ s}^{-1}$) were achieved for reactions between dibenzocyclooctyne derivatives and azides.^{23b} The inverse-electron-demand (4 + 2) cycloadditions of tetrazine and *trans*-cyclooctene have rate constants as high as $10^4 \text{ M}^{-1} \text{ s}^{-1}$.¹⁴ These two types of bioorthogonal cycloadditions are mutually orthogonal, as shown earlier in Figure 3, and were successfully used to label two different cancer cell types in biological environments simultaneously.^{24a} The concept of mutual orthogonality is an important one in chemical biology. When two reactions are both bioorthogonal and do not interfere with each other, then they can be used to enable labeling and imaging of several proteins or metabolic substrates simultaneously.^{24b,c} To understand the factors controlling mutual orthogonality, we studied the reactions shown in Figure 9.⁸ Electron-deficient dimethyltetrazine reacts faster with the parent *trans*-cyclooctene and cyclooctyne than does methyl azide (**TS12** and **TS13** in Figure 9) but much slower in the case of dibenzocyclooctyne (**TS14**), just as observed in experiments. The calculated activation barriers, relative rate constants, and D/I analyses are shown below each structure.

The interaction energies (Figure 9) for tetrazine cycloadditions are always around 10 kcal/mol more favorable than those for azide reactions. Frontier molecular orbital analysis showed that the lower-lying interacting orbital of tetrazine (LUMO+1 = 2.5 eV) compared with azide (LUMO = 3.4 eV) is the origin of its intrinsic high electrophilic reactivity. The sterically hindered dibenzocyclooctyne, however, reduces the reactivity with tetrazine by introducing additional distortion energies (**TS14b**; Figure 9). We therefore proposed a general principle in designing mutually orthogonal reaction pairs—intrinsically more reactive substances can be made less reactive by increasing the distortion controlled by steric effects. On the basis of this principle, we predicted that methylcyclopropene and 3,3,6,6-tetramethylthiacycloheptyne (TMTH) should be orthogonal in reactions with azide and tetrazine. Figure 10 shows the predicted relative rate constants for these reactions, suggesting that tetrazines will react readily with 1-alkylcyclopropenes but not the bulky thiacyclooctyne, while azides will exhibit the opposite reactivity.

A wonderful coincidence of interests occurred soon after our prediction was published in *JACS*,⁸ when the reactions of 1-alkylcyclopropenes with tetrazines were used as bioorthogonal and mutually orthogonal cycloadditions and reported by the Prescher group in *JACS* only a few weeks after our paper.²⁵ We were both excited about the results and started our collaborations on tetrazine and triazine bioorthogonal chemistry.

3. Cyclopropene Reactivities in Bioorthogonal Cycloadditions with Tetrazines

A variety of substituted cyclopropene analogues were synthesized by the Prescher²⁵ and Devaraj²⁶ groups. These cyclopropenes were found to be stable in a biological environment. Multisubstituted cyclopropenes show orthogonal reactivities toward tetrazines and nitrile imines, suggesting their utility for studies of multiple biomolecules in succession (Figure 11). While 1,3-disubstituted cyclopropenes react rapidly and selectively with tetrazines,^{25,26} 3,3-disubstituted cyclopropenes preferentially participate in 1,3-dipolar cycloadditions with nitrile imines, which are generated through cycloreversion reactions of tetrazoles that release N₂.²⁷

We studied the model reactions (Figure 12) with DFT calculations, and the computed reactivities agree well with the kinetic data obtained from experiments.^{21a} The calculated activation barriers and relative rate constants are shown in Figure 12. The sterically less encumbered nitrile imine is less sensitive to the steric effect at C3 of cyclopropene. The calculated rate constants for the reactions of nitrile imine with 1,3- and 3,3-disubstituted cyclopropenes are about the same because of almost identical distortion energies and very similar interaction energies (**TS15a** and **TS16a**; Figure 12). On the contrary, the placement of a methyl group at C3 of cyclopropene significantly reduces its reactivity with tetrazine by over 4 orders of magnitude. The methyl group prevents the ideal alignment of the reacting partners and causes them to distort. An increase in distortion energy and a decrease in stabilizing interaction energy were observed in going from **TS15b** to **TS16b** (Figure 12).

The D/I analysis of orthogonality predicted the application of two pairs of cycloadditions in multicomponent imaging, where tetrazine probes selectively ligate with 1,3-dimethylcyclopropenes and the unreacted 3,3-dimethylcyclopropenes can then ligate with nitrile imines added in a second operation.

4. Substituent Effects in Tetrazine Cyclopropene Ligations

Cyclopropenes quickly attracted enormous attention after their introduction as bioorthogonal reporters because of their small sizes, biocompatibility, and cycloaddition reactivities. Our group and the Devaraj group followed up on the substituent effects on tetrazine–cyclopropene ligation and successfully identified the origin of the variation in reactivity with the D/I model.²⁸

A series of 1-methyl-3-substituted cyclopropenes with different functional groups were synthesized and tested. The second-order rate constants for the reactions of these cyclopropenes with tetrazine range from 10^{-3} to $1 \text{ M}^{-1} \text{ s}^{-1}$ both computationally and experimentally, as shown in Figure 13. The differences in the reactivities of various cyclopropenes are dominated by the changes in the interaction energies. Electron-donating groups increase the HOMO energies of cyclopropenes and shrink the energy gaps with the vacant π^* orbital of tetrazine, leading to lower activation barriers.

Cyclopropenes are not sensitive to steric hindrance of the probe, while the strain-promoted alkene champion, *trans*-cyclooctene, is intrinsically more reactive than cyclopropene in reactions with tetrazines but becomes less reactive when reacting with sterically hindered yet extremely stable *tert*-butyltetrazine.

5. Bioorthogonal Cycloadditions of Triazines

Tetrazines have excellent reactivities in bioorthogonal cycloadditions with *trans*-cyclooctenes and cyclopropenes but also undergo reactions with water and nucleophiles. To overcome this, we expanded our studies of electron-deficient dienes to triazine species. We predicted that 1,2,4-triazines would be less reactive than tetrazines but still effective in cycloaddition reactions with activated alkenes.²⁹ Our collaborators, the Prescher group at UCI, tested the biological stability of 1,2,4-triazines and confirmed their potential as a new class of bioorthogonal reagents.^{21b}

The decrease in reactivity in going from tetrazine to triazine, as shown in the D/I analysis of their reactions with ethylene, comes from the decrease in interaction energy and increase in distortion energy. To achieve better overlap of the interacting orbitals, 1,2,4-triazine has to distort more to achieve the transition state than 1,2,4,5-tetrazine (Figure 14). The intrinsic reactivity of triazine can be tuned by installing different substituents. We showed that various aryl groups at C6 can alter the rate constant for the triazine–*trans*-cyclooctene ligation by 1 order of magnitude.^{21b}

Figure 15 shows that 5-phenyl-1,2,4-triazine has a much higher reactivity than 6-phenyl-1,2,4-triazine and 3,6-diphenyl-1,2,4,5-tetrazine in reactions with sterically hindered dienophiles such as TMTH. With a sterically unencumbered cyclopropene, by contrast, the tetrazine is much more reactive. Our theoretical predictions were proven experimentally by the Prescher group. 5-Phenyl-1,2,4-triazine reacts with TMTH rapidly with a second-order rate constant of $0.22 \text{ M}^{-1} \text{ s}^{-1}$, while 6-phenyl-1,2,4-triazine and 3,6-diphenyltetrazine show no reactivity toward TMTH.³⁰

6. Computational-Guided Discovery of Bioorthogonal Reactions of Sydnone

In order to explore extraordinarily complex biological processes, new bioorthogonal and mutually orthogonal reactions are needed. Many groups are developing new bioorthogonal reactions with appropriately high rate constants and selectivities. Experimental screening is time-consuming, but we have developed a computational screening process that led to the prediction of the high reactivity of sydnones with two distortion-promoted dibenzocyclooctyne analogues (DIBAC and BARAC).^{21e}

The mesoionic structure of sydnones was first discovered in 1935,³¹ but it was about 30 years later when Huisgen reported the (3 + 2) cycloadditions of sydnones with alkynes to form pyrazoles.³² Widely used as a powerful tool in the synthesis of heterocyclic compounds, the 1,3-dipolar cycloaddition of sydnone was recently applied to bioorthogonal chemistry. Taran and co-workers reported the highly efficient and selective copper-catalyzed cycloadditions of sydnone with terminal alkynes³³ and demonstrated the satisfying biocompatibility of such reactions. Wallace and Chin^{21d} improved the reaction by introducing the strain-promoted cyclooctyne, bicyclo[6.1.0]-nonyne (BCN), which reacts with *N*-phenylsydnone at ambient temperature with a rate constant of $0.054 \text{ M}^{-1} \text{ s}^{-1}$.

Our group computationally screened a variety of reactions of *N*-phenylsydnone with a series of distortion-promoted alkenes and alkynes (Figure 16). DIBAC and BARAC show even better reactivities than BCN; the rate constants of the two reactions are predicted to be 1 and $10 \text{ M}^{-1} \text{ s}^{-1}$, respectively. By contrast, norbornene was found to be the least reactive with sydnone. We predicted that two pairs of orthogonal reactions could be applied to probe multiple biomolecules. Our collaborators, the group of Jennifer Murphy at UCLA, confirmed this prediction and successfully labeled two proteins, bovine serum albumin and ovalbumin, simultaneously (Figure 17).^{21e}

7. Computational Screening of New Bioorthogonal Cycloadditions

This Account has described the development of a theoretical understanding of a variety of cycloadditions, using the distortion/interaction model to help extract information on factors that control reactivities. Given the wealth of information about which diene, 1,3-dipole, and dienophile or dipolarophile are bioorthogonal, the number of possible combinations of reactions that might be used to probe biology is enormous! It would be very useful to know in advance what the rate constants for each of these reactions will be and to screen hundreds of potential reactions in advance of experiments.

We have begun to amass exactly such information by performing computational predictions of second-order rate constants for reactions in water at room temperature. The rate constants are derived from calculated activation barriers corrected with the calibration formula shown in Figure 6. Figure 18 gives a “heat map” or “reactivity matrix” of predicted rate constants (in $\text{M}^{-1} \text{ s}^{-1}$) for 121 reactions of 11 1,3-dipoles/dienes with 11 dipolarophiles/dienophiles. The map is color-coded according to the calculated rate constants.

Comparisons of experimental rates for typical cases to the predicted rate constants in Figure 18 show that our predictions are within an order of magnitude of the experimental rate constants. For example, the reactions of azide with cyclooctyne species were observed to

have second-order rate constants within the range of 10^{-3} to $10^{-1} \text{ M}^{-1} \text{ s}^{-1}$, in excellent agreement with our calculations. Diphenyltetrazine has been shown to react more rapidly with dienophiles than dimethyltetrazine by about 1 order of magnitude. A detailed discussion of the substituent effects on tetrazine was reported by our group.³⁴ Recently, triazine was proposed and tested as a bioorthogonal reactant,^{21b} and 5-substituted triazines have better reactivities than 3- or 6-substituted triazines toward sterically encumbered dienophiles such as TMTM.³⁰ All of the functionalities in Figure 18 have been used in bioorthogonal chemistry, so we know that compounds with these reactive groups will indeed be bioorthogonal, allowing applications in actual cellular milieu.

A great advantage of this reactivity matrix is that it provides a convenient way to design new mutually orthogonal reaction pairs. The dashed rectangle at the middle left of Figure 18 shows the mutual orthogonality of methyl azide and dimethyltetrazine with *trans*-cyclooctene and dibenzocyclooctyne (as discussed earlier in this Account). Methyl azide reacts rapidly with dibenzocyclooctyne but slowly with *trans*-cyclooctene; on the contrary, dimethyltetrazine is highly reactive toward *trans*-cyclooctene but inert toward dibenzocyclooctyne. On the reactivity matrix, mutual orthogonality requires two boxes on two opposing corners (one diagonal) of the rectangle to be green, while those on the other two corners are red. We mark these corners with green and red circles, respectively, to indicate that they represent mutually orthogonal pairs. With such general guidelines, we are able to predict other mutually orthogonal reactions: for a given column (one 4π cycloaddend), we scan down the column to find a green box and a red box, and then we scan across those two rows to look for red and green complementary boxes in the same column. One example is shown by the smaller dashed rectangle in Figure 18—sydnone and diaryltetrazine reacting with dibenzocyclooctyne and norbornene (for details, see Figure 17). The actual reagents to be used will be substituted versions of those in our reactivity matrix.

IV. CONCLUSION

The development of bioorthogonal cycloadditions has been extraordinarily rapid in the 21st century since click chemistry began to be used for these purposes. The contributions of computations to this field began in the past decade and have matured as computations have become a full partner with experiment for understanding and discovery.

Acknowledgments

We are grateful to the National Science Foundation (CHE-1361104) and the National Institute of General Medical Sciences, National Institutes of Health (R01 GM109078) for financial support of this research. Y.L. thanks the National Thousand Young Talents Program and the Jiangsu Specially-Appointed Professor Plan in China for support.

Biographies

Fang Liu received her B.S. in chemistry from Nankai University, China, in 2009. She came to UCLA as part of the CSST Program and received her Ph.D. with K. N. Houk at UCLA in 2014, studying gating in container molecules and the factors controlling reactivity in bioorthogonal cycloadditions. After a postdoctoral fellowship in the Houk group, she has continued as a postdoctoral fellow in the Liang group at Nanjing University.

Yong Liang received his B.S. (2005) and Ph.D. (2010) at Peking University, working with Jiayi Xu as an undergraduate and Zhi-Xiang Yu as a graduate student in the field of synthetic and computational organic chemistry. After a postdoctoral fellowship in the Houk group at UCLA, he joined the faculty of the School of Chemistry and Chemical Engineering at Nanjing University in 2015. His main research interests are to understand reaction mechanisms and the factors controlling the reactivity and selectivity of important chemical transformations.

K. N. Houk is the Saul Winstein Chair in Organic Chemistry at UCLA. He is a computational organic chemist. He received his Ph.D. at Harvard with R. B. Woodward in 1968, doing experimental work in orbital-symmetry-predicted chemistry. He has published extensively on pericyclic reactions, stereoselectivity, molecular recognition, and enzyme design. He is a Fellow of the American Academy of Arts and Sciences and a Member of the National Academy of Sciences.

References

1. (a) Kobayashi, S., Jorgensen, KA. Cycloaddition Reactions in Organic Synthesis. Wiley-VCH; Weinheim, Germany: 2001. (b) Nishiwaki, N. Methods and Applications of Cycloaddition Reactions in Organic Synthesis. Wiley-VCH; Weinheim, Germany: 2014. (c) Nicolaou KC, Vourloumis D, Winssinger N, Baran PS. The Art and Science of Total Synthesis. *Angew. Chem. Int. Ed.* 2000; 39:44–122.
2. Huisgen R. 1,3-Dipolar Cycloadditions. Past and Future. *Angew. Chem. Int. Ed. Engl.* 1963; 2:565–632.
3. Diels O, Alder K. Synthesen in der Hydroaromatischen Reihe. *Justus Liebigs Annalen der Chemie.* 1928; 460:98.
4. (a) Houk KN, Sims J, Duke RE Jr, Strozier RW, George JK. Frontier Molecular Orbitals of 1,3-Dipoles and Dipolarphiles. *J. Am. Chem. Soc.* 1973; 95:7287–7300. (b) Houk KN, Sims J, Watts CR, Luskus LJ. The Origin of Reactivity, Regioselectivity, and Periselectivity in 1,3-Dipolar Cycloadditions. *J. Am. Chem. Soc.* 1973; 95:7301–7315. (c) Houk KN. Frontier Molecular Orbital Theory of Cycloaddition Reactions. *Acc. Chem. Res.* 1975; 8:361–369. (d) Houk, KN. *Organic Chemistry*. Springer; Berlin: 1979. Theoretical and Experimental Insights into Cycloaddition Reactions; p. 1-40. (e) Houk, KN., Yamaguchi, K. Theory of 1,3-Dipolar Cycloadditions. In: Padwa, A., editor. *1,3-Dipolar Cycloaddition Chemistry*. Vol. 2. Wiley; New York: 1984. p. 407-450. (f) Ess DH, Jones GO, Houk KN. Conceptual, Qualitative, and Quantitative Theories of 1,3-Dipolar and Diels–Alder Cycloadditions Used in Synthesis. *Adv. Synth. Catal.* 2006; 348:2337–2361.
5. (a) Ess DH, Houk KN. Distortion/Interaction Energy Control of 1,3-Dipolar Cycloaddition Reactivity. *J. Am. Chem. Soc.* 2007; 129:10646–10647. [PubMed: 17685614] (b) Ess DH, Houk KN. Theory of 1,3-Dipolar Cycloadditions: Distortion/Interaction and Frontier Molecular Orbital Models. *J. Am. Chem. Soc.* 2008; 130:10187–10198. [PubMed: 18613669]
6. (a) Fernandez I, Bickelhaupt FM. The activation strain model and molecular orbital theory: understanding and designing chemical reactions. *Chem. Soc. Rev.* 2014; 43:4953–4967. [PubMed: 24699791] (b) Wolters LP, Bickelhaupt FM. The activation strain model and molecular orbital theory. *Wiley Interdisciplinary Reviews: Computational Molecular Science.* 2015; 5:324–343. [PubMed: 26753009] (c) Fernandez, I. *Discovering the Future of Molecular Science, Understanding Trends in Reaction Barriers*. Pignataro, B., editor. Wiley-VCH; Weinheim, Germany: 2014. p. 165-187.
7. (a) Paton RS, Kim S, Ross AG, Danishefsky SJ, Houk KN. Experimental Diels–Alder Reactivities of Cycloalkenones and Cyclic Dienes Explained through Transition-State Distortion Energies. *Angew. Chem. Int. Ed.* 2011; 50:10366–10368. (b) Liu F, Paton RS, Kim S, Liang Y, Houk KN. Diels–Alder Reactivities of Strained and Unstrained Cycloalkenes with Normal and Inverse-Electron-Demand Dienes: Activation Barriers and Distortion/Interaction Analysis. *J. Am. Chem.*

- Soc. 2013; 135:15642–15649. [PubMed: 24044412] (c) Levandowski BJ, Hamlin TA, Bickelhaupt FM, Houk KN. Role of orbital interactions and activation strain (distortion energies) on reactivities in the normal and inverse electron-demand cycloadditions of strained and unstrained cycloalkenes. *J. Org. Chem.* 2017; 82:8668–8675. [PubMed: 28712288]
8. Liang Y, Mackey JL, Lopez SA, Liu F, Houk KN. Control and Design of Mutual Orthogonality in Bioorthogonal Cycloadditions. *J. Am. Chem. Soc.* 2012; 134:17904–17907. [PubMed: 23061442]
 9. (a) Vocadlo DJ, Hang HC, Kim E-J, Hanover JA, Bertozzi CR. A chemical approach for identifying O-GlcNAc-modified proteins in cells. *Proc. Natl. Acad. Sci. U. S. A.* 2003; 100:9116–9121. [PubMed: 12874386] (b) Shieh P, Bertozzi CR. Design strategies for bioorthogonal smart probes. *Org. Biomol. Chem.* 2014; 12:9307–9320. [PubMed: 25315039] (c) Lang K, Chin JW. Bioorthogonal Reactions for Labeling Proteins. *ACS Chem. Biol.* 2014; 9:16–20. [PubMed: 24432752] (d) Lang K, Chin JW. Cellular Incorporation of Unnatural Amino Acids and Bioorthogonal Labeling of Proteins. *Chem. Rev.* 2014; 114:4764–4806. [PubMed: 24655057] (e) Shih H-W, Kamber DN, Prescher JA. Building better bioorthogonal reactions. *Curr. Opin. Chem. Biol.* 2014; 21:103–111. [PubMed: 25086220] (f) Patterson DM, Nazarova LA, Prescher JA. Finding the Right (Bioorthogonal) Chemistry. *ACS Chem. Biol.* 2014; 9:592–605. [PubMed: 24437719] (g) King M, Wagner A. Developments in the Field of Bioorthogonal Bond Forming Reactions—Past and Present Trends. *Bioconjugate Chem.* 2014; 25:825–839.
 10. Kalia J, Raines RT. Advances in Bioconjugation. *Curr. Org. Chem.* 2010; 14:138–147. [PubMed: 20622973]
 11. Saxon E, Bertozzi CR. Cell Surface Engineering by a Modified Staudinger Reaction. *Science.* 2000; 287:2007. [PubMed: 10720325]
 12. Agard NJ, Prescher JA, Bertozzi CR. A Strain-Promoted [3 + 2] Azide-Alkyne Cycloaddition for Covalent Modification of Biomolecules in Living Systems. *J. Am. Chem. Soc.* 2004; 126:15046–15047. [PubMed: 15547999]
 13. (a) Rostovtsev VV, Green LG, Fokin VV, Sharpless KB. A Stepwise Huisgen Cycloaddition Process: Copper(I)-Catalyzed Regioselective “Ligation” of Azides and Terminal Alkynes. *Angew. Chem. Int. Ed.* 2002; 41:2596–2599. (b) Presolski SI, Hong V, Cho S-H, Finn MG. Tailored Ligand Acceleration of the Cu-Catalyzed Azide–Alkyne Cycloaddition Reaction: Practical and Mechanistic Implications. *J. Am. Chem. Soc.* 2010; 132:14570–14576. [PubMed: 20863116]
 14. (a) Blackman ML, Royzen M, Fox JM. Tetrazine Ligation: Fast Bioconjugation Based on Inverse-Electron-Demand Diels–Alder Reactivity. *J. Am. Chem. Soc.* 2008; 130:13518–13519. [PubMed: 18798613] (b) Devaraj NK, Weissleder R, Hilderbrand SA. Tetrazine-Based Cycloadditions: Application to Pretargeted Live Cell Imaging. *Bioconjugate Chem.* 2008; 19:2297–2299.
 15. Nagase S, Morokuma K. An ab initio molecular orbital study of organic reactions. The energy, charge, and spin decomposition analyses at the transition state and along the reaction pathway. *J. Am. Chem. Soc.* 1978; 100:1666–1672.
 16. (a) Ziegler T, Rauk A. On the calculation of bonding energies by the Hartree Fock Slater method. *Theoretica chimica acta.* 1977; 46:1–10. (b) Santiago C, Gandour RW, Houk KN, Nutakul W, Cravey WE, Thummel RP. Photoelectron and ultraviolet spectra of small-ring fused aromatic molecules as probes of aromatic ring distortions. *J. Am. Chem. Soc.* 1978; 100:3730–3737. (c) Strozier RW, Caramella P, Houk KN. Influence of molecular distortions upon reactivity and stereochemistry in nucleophilic additions to acetylenes. *J. Am. Chem. Soc.* 1979; 101:1340–1343. (d) Rondan NG, Domelsmith LN, Houk KN, Bowne AT, Levin RH. The relative rates of electron-rich and electron-deficient alkene cycloadditions to benzyne. Enhanced electrophilicity as a consequence of alkyne bending distortions. *Tetrahedron Lett.* 1979; 20:3237–3240. (e) Houk, KN. Molecular Distortions and Organic Reactivity: Additions, Cycloadditions, and Free Radical Reactions. In: Pryor, WA., editor. *Frontiers of Free Radical Chemistry.* Academic Press; New York: 1980. (f) Rondan NG, Paddon-Row MN, Caramella P, Houk KN. Nonplanar alkenes and carbonyls: a molecular distortion which parallels addition stereoselectivity. *J. Am. Chem. Soc.* 1981; 103:2436–2438.
 17. Bickelhaupt FM, Houk KN. Distortion/Interaction- Activation Strain Model to Analyze Reaction Rates. *Angew. Chem. Int. Ed.* 2017; 56:10070.
 18. Frisch, MJ., et al. *Gaussian 09 Revision D.01.* Gaussian, Inc.; Wallingford, CT: 2009.

19. (a) Zhao Y, Truhlar DG. The M06 suite of density functionals for main group thermochemistry, thermochemical kinetics noncovalent interactions, excited states, and transition elements: two new functionals and systematic testing of four M06-class functionals and 12 other functionals. *Theor. Chem. Acc.* 2008; 120:215–241. (b) Zhao Y, Truhlar DG. Density Functionals with Broad Applicability in Chemistry. *Acc. Chem. Res.* 2008; 41:157–167. [PubMed: 18186612]
20. (a) Barone V, Cossi M. Quantum Calculation of Molecular Energies and Energy Gradients in Solution by a Conductor Solvent Model. *J. Phys. Chem. A.* 1998; 102:1995–2001. (b) Cossi M, Rega N, Scalmani G, Barone V. Energies, structures, and electronic properties of molecules in solution with the C-PCM solvation model. *J. Comput. Chem.* 2003; 24:669–681. [PubMed: 12666158]
21. (a) Kamber DN, Nazarova LA, Liang Y, Lopez SA, Patterson DM, Shih H-W, Houk KN, Prescher JA. Isomeric Cyclopropenes Exhibit Unique Bioorthogonal Reactivities. *J. Am. Chem. Soc.* 2013; 135:13680–13683. [PubMed: 24000889] (b) Kamber DN, Liang Y, Blizzard RJ, Liu F, Mehl RA, Houk KN, Prescher JA. 1,2,4-Triazines Are Versatile Bioorthogonal Reagents. *J. Am. Chem. Soc.* 2015; 137:8388–8391. [PubMed: 26084312] (c) Ning X, Temming RP, Dommerholt J, Guo J, Ania DB, Debets MF, Wolfert MA, Boons G-J, van Delft FL. Protein Modification by Strain-Promoted Alkyne–Nitrone Cycloaddition. *Angew. Chem. Int. Ed.* 2010; 49:3065–3068. (d) Wallace S, Chin JW. Strain-promoted sydnone bicyclo-[6.1.0]-nonyne cycloaddition. *Chem. Sci.* 2014; 5:1742–1744. [PubMed: 25580211] (e) Narayanam MK, Liang Y, Houk KN, Murphy JM. Discovery of new mutually orthogonal bioorthogonal cycloaddition pairs through computational screening. *Chem. Sci.* 2016; 7:1257–1261.
22. (a) Baskin JM, Prescher JA, Laughlin ST, Agard NJ, Chang PV, Miller IA, Lo A, Codelli JA, Bertozzi CR. Copper-free click chemistry for dynamic in vivo imaging. *Proc. Natl. Acad. Sci. U. S. A.* 2007; 104:16793–16797. [PubMed: 17942682] (b) Ning X, Guo J, Wolfert MA, Boons G-J. Visualizing Metabolically Labeled Glycoconjugates of Living Cells by Copper-Free and Fast Huisgen Cycloadditions. *Angew. Chem. Int. Ed.* 2008; 47:2253–2255. (c) Debets MF, van Berkel SS, Schoffelen S, Rutjes FPJT, van Hest JCM, van Delft FL. Aza-dibenzocyclooctynes for fast and efficient enzyme PEGylation via copper-free (3 + 2) cycloaddition. *Chem. Commun.* 2010; 46:97–99. (d) Jewett JC, Sletten EM, Bertozzi CR. Rapid Cu-Free Click Chemistry with Readily Synthesized Biarylazacyclooctynones. *J. Am. Chem. Soc.* 2010; 132:3688–3690. [PubMed: 20187640]
23. (a) Ess DH, Jones GO, Houk KN. Transition states of strain-promoted metal-free click chemistry: 1,3-dipolar cycloadditions of phenyl azide and cyclooctynes. *Org. Lett.* 2008; 10:1633–1636. [PubMed: 18363405] (b) Gordon CG, Mackey JL, Jewett JC, Sletten EM, Houk KN, Bertozzi CR. Reactivity of Biarylazacyclooctynones in Copper-Free Click Chemistry. *J. Am. Chem. Soc.* 2012; 134:9199–9208. [PubMed: 22553995]
24. (a) Karver MR, Weissleder R, Hilderbrand SA. Bioorthogonal Reaction Pairs Enable Simultaneous, Selective, Multi-Target Imaging. *Angew. Chem. Int. Ed.* 2012; 51:920–922. (b) Cole CM, Yang J, Še kut J, Devaraj NK. Fluorescent live-cell imaging of metabolically incorporated unnatural cyclopropene-mannosamine derivatives. *ChemBioChem.* 2013; 14:205–208. [PubMed: 23292753] (c) Sachdeva A, Wang K, Elliott T, Chin JW. Concerted, rapid, quantitative, and site-specific dual labeling of proteins. *J. Am. Chem. Soc.* 2014; 136:7785–7788. [PubMed: 24857040]
25. Patterson DM, Nazarova LA, Xie B, Kamber DN, Prescher JA. Functionalized Cyclopropenes as Bioorthogonal Chemical Reporters. *J. Am. Chem. Soc.* 2012; 134:18638–18643. [PubMed: 23072583]
26. Yang J, Še kut J, Cole CM, Devaraj NK. Live-Cell Imaging of Cyclopropene Tags with Fluorogenic Tetrazine Cycloadditions. *Angew. Chem. Int. Ed.* 2012; 51:7476–7479.
27. Yu Z, Pan Y, Wang Z, Wang J, Lin Q. Genetically Encoded Cyclopropene Directs Rapid, Photoclick-Chemistry-Mediated Protein Labeling in Mammalian Cells. *Angew. Chem. Int. Ed.* 2012; 51:10600–10604.
28. Yang J, Liang Y, Še kut J, Houk KN, Devaraj NK. Synthesis and Reactivity Comparisons of 1-Methyl-3-Substituted Cyclopropene Mini-tags for Tetrazine Bioorthogonal Reactions. *Chem. - Eur. J.* 2014; 20:3365–3375. [PubMed: 24615990]
29. Yang Y-F, Liang Y, Liu F, Houk KN. Diels–Alder Reactivities of Benzene, Pyridine, and Di-, Tri-, and Tetrazines: The Roles of Geometrical Distortions and Orbital Interactions. *J. Am. Chem. Soc.* 2016; 138:1660–1667. [PubMed: 26804318]

30. Kamber D, Nguyen S, Liang Y, Liu F, Briggs J, Shih H-W, Houk KN, Prescher J. Isomeric 1,2,4-triazines exhibit distinct profiles of bioorthogonal reactivity. Submitted.
31. Earl JC, Mackney AW. 204. The action of acetic anhydride on N-nitrosophenylglycine and some of its derivatives. *J. Chem. Soc.* 1935:899–900.
32. Huisgen R, Grashey R, Gotthardt H, Schmidt R. 1,3-Dipolar Additions of Sydnone to Alkynes. A New Route into the Pyrazole Series. *Angew. Chem. Int. Ed. Engl.* 1962; 1:48–49.
33. Kolodych S, Rasolofonjatovo E, Chaumontet M, Nevers M-C, Créminon C, Taran F. Discovery of Chemoselective and Biocompatible Reactions Using a High-Throughput Immunoassay Screening. *Angew. Chem. Int. Ed.* 2013; 52:12056–12060.
34. Liu F, Liang Y, Houk KN. Theoretical Elucidation of the Origins of Substituent and Strain Effects on the Rates of Diels–Alder Reactions of 1,2,4,5-Tetrazines. *J. Am. Chem. Soc.* 2014; 136:11483–11493. [PubMed: 25041719]

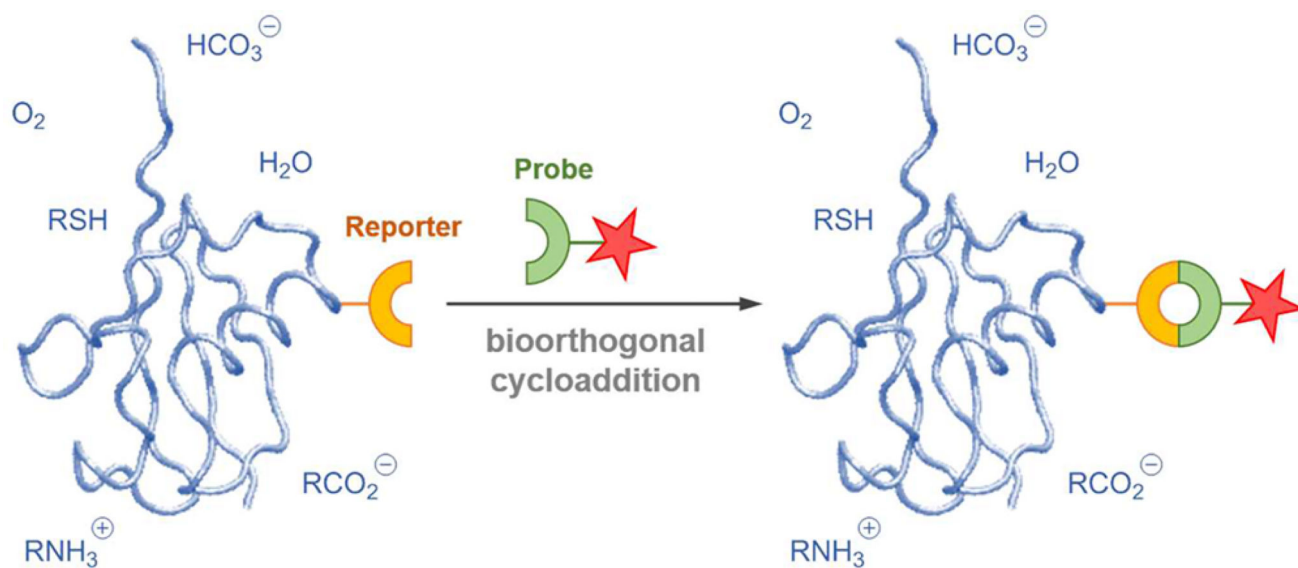


Figure 1. Representative bioorthogonal cycloaddition. The probe and reporter contain functional groups that undergo a cycloaddition to form a new ring, represented by the circle in the product.

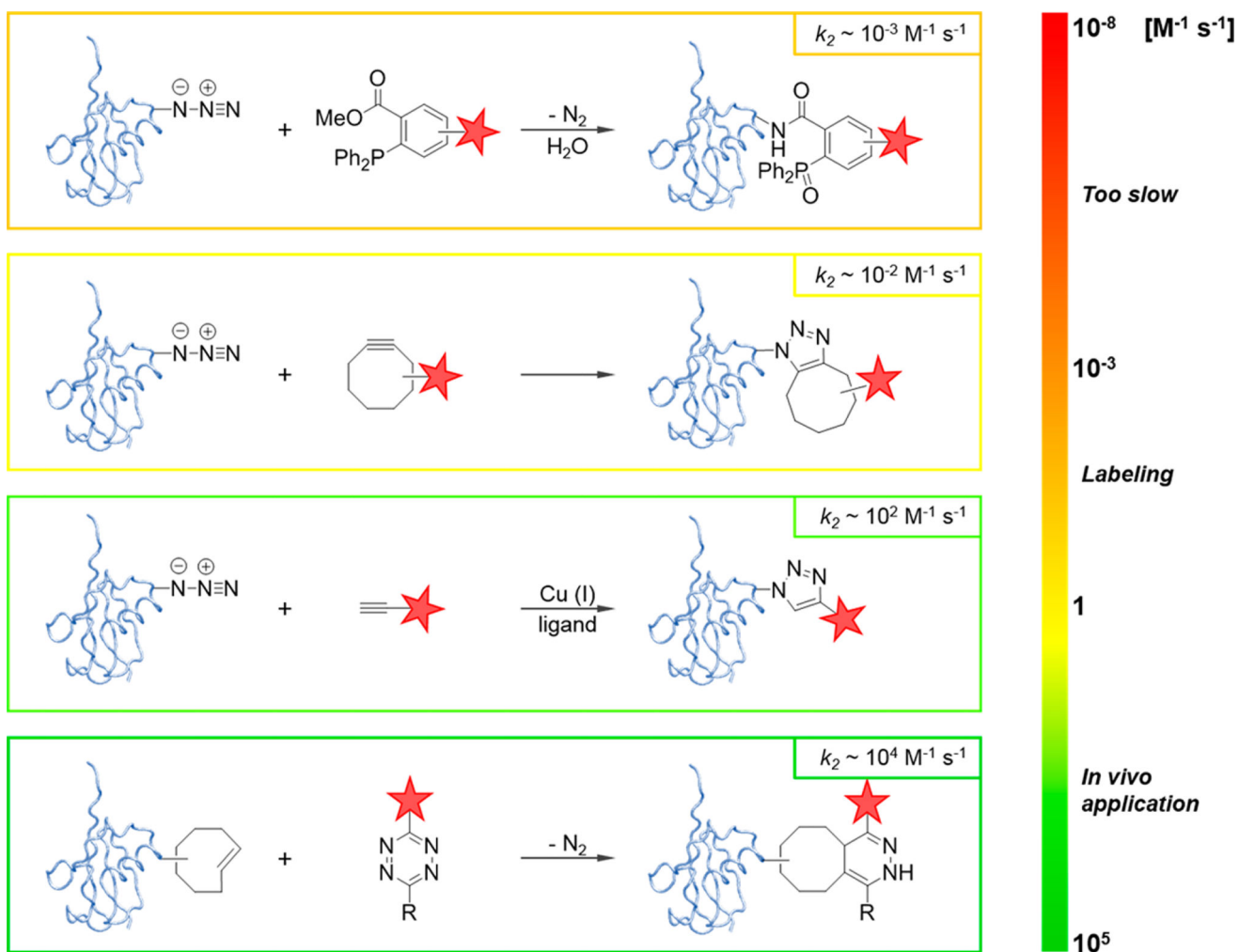
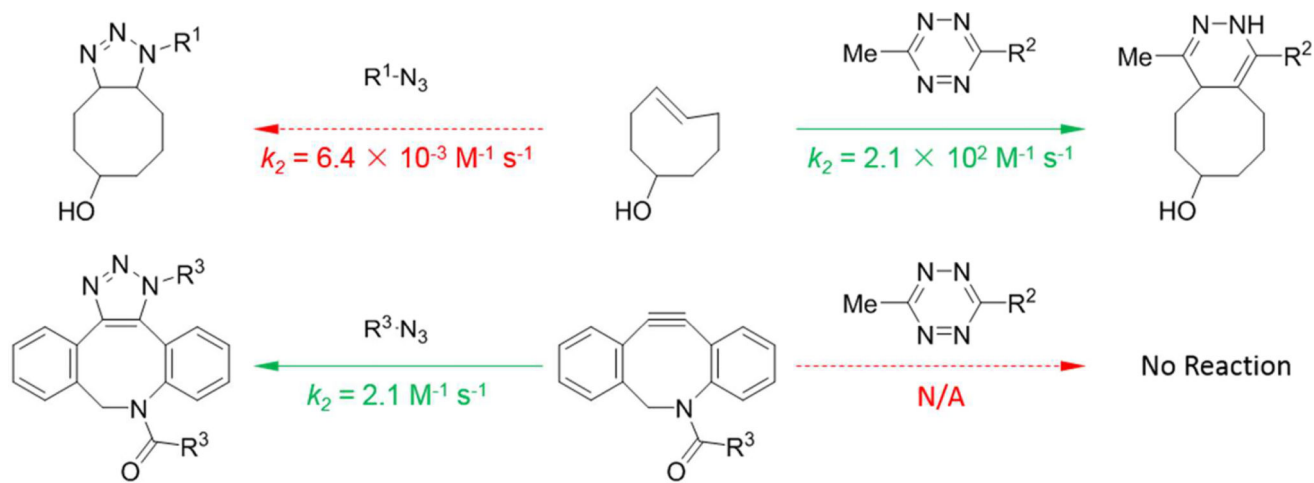


Figure 2. Range of rate constants for various examples of bioorthogonal reactions. The first is the Staudinger ligation, one of the first bioorthogonal reactions developed by the Bertozzi group, and the other three reactions are later-developed bioorthogonal cycloadditions.

**Figure 3.**

Examples of bioorthogonal cycloadditions that are also mutually orthogonal. $\text{R}^1\text{-N}_3$ = Alexa Fluor 647 azide; R^2 = $(\text{CH}_2)_5\text{NH}_2$; R^3 = PEG4- CO_2H .

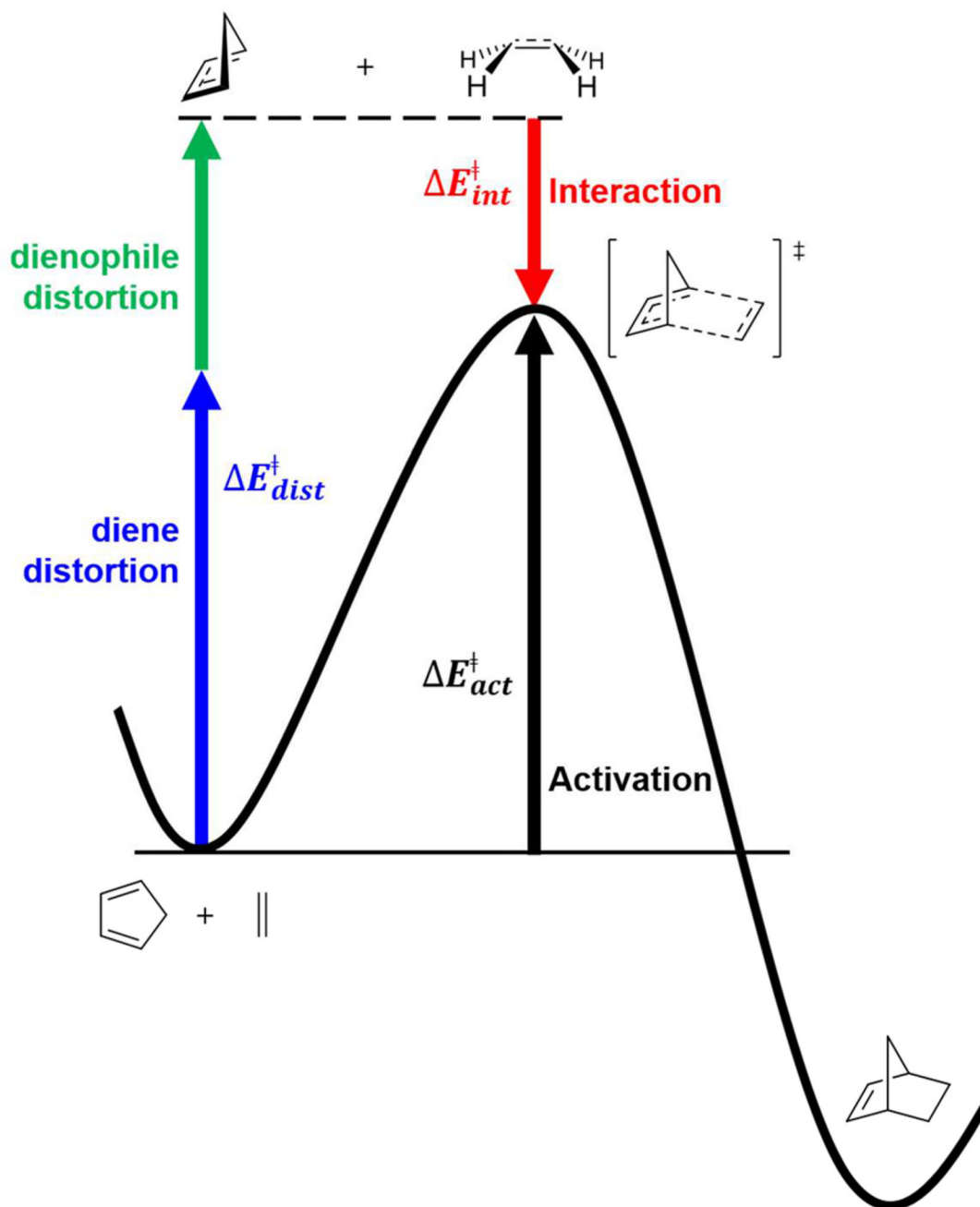


Figure 4. D/I model. Black arrow, activation energy; red arrow, interaction energy; blue and green arrows, distortion energies of the diene and dienophile, respectively.

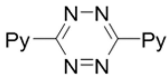

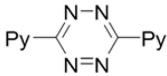
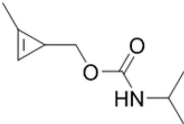
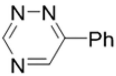
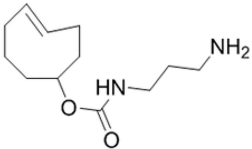
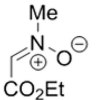
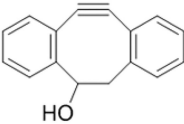
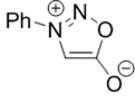
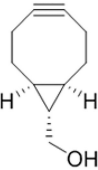
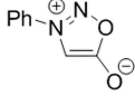
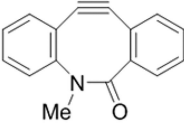
Entry	4 π -component	2 π -component	k_2 (M ⁻¹ s ⁻¹)	condition	Reference
1			2000	9:1 MeOH/H ₂ O, 25 °C	14a
2			2.8	15% DMSO/PBS	21a
3			0.034	CD ₃ CN/ <i>d</i> -PBS	21b
4			3.9	3:1 CH ₃ CN/H ₂ O	21c
5			0.054	55:45 MeOH/H ₂ O, 21 °C	21d
6			1.5	1:1 CH ₃ CN/H ₂ O, 23 °C	21e

Figure 5. Experimentally measured second-order rate constants for six bioorthogonal cycloadditions.^{14a,21}

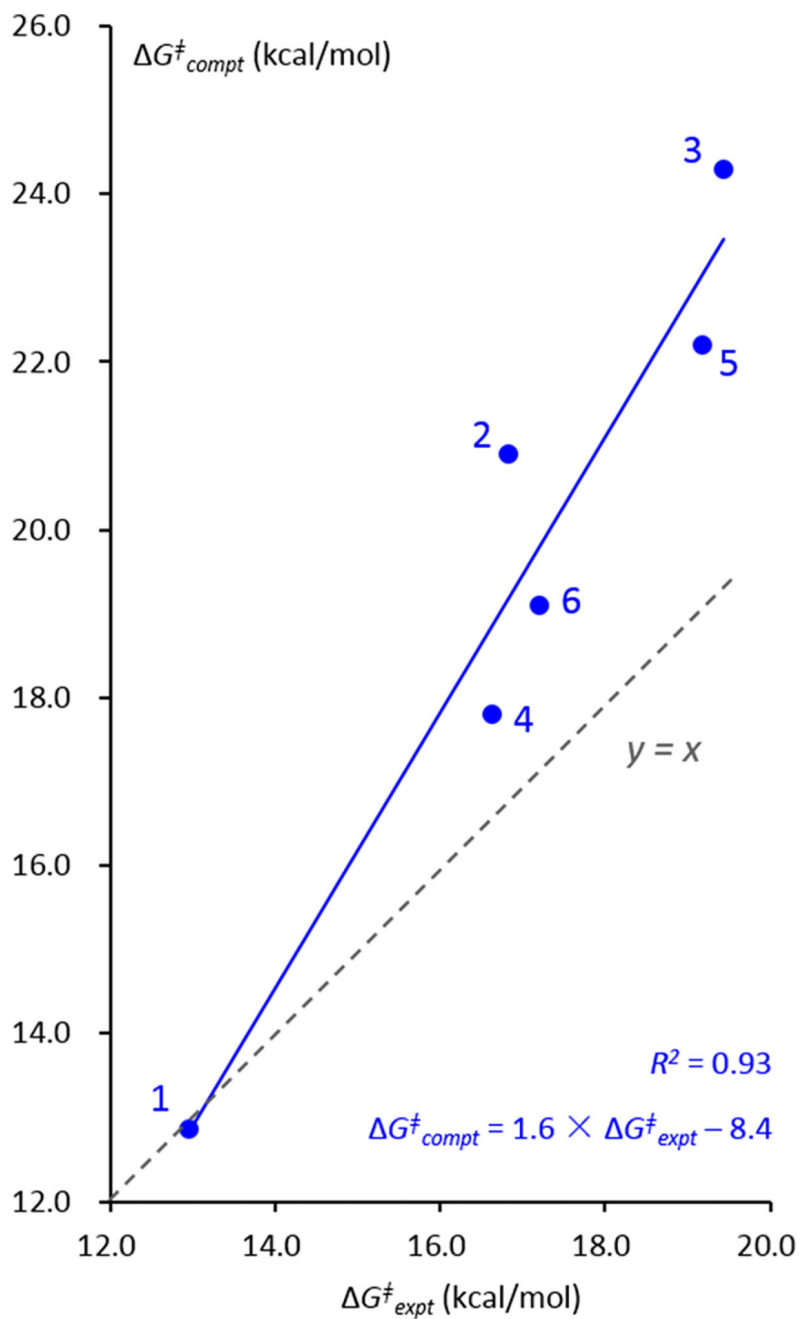
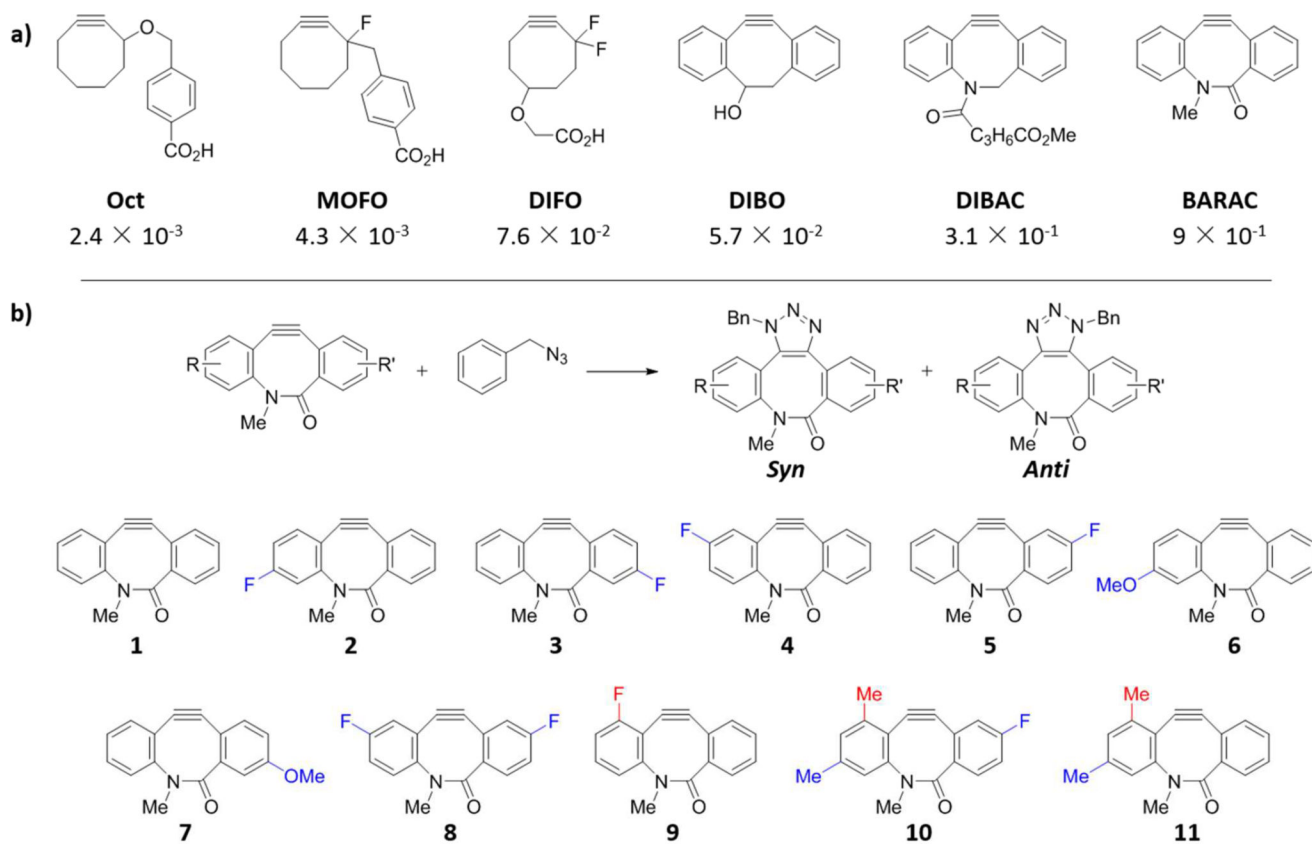


Figure 6.

Computed activation free energies ($\Delta G_{\text{compt}}^{\ddagger}$) correlate well with experimentally observed values ($\Delta G_{\text{expt}}^{\ddagger}$).

**Figure 7.**

(a) Cyclooctynes and dibenzo analogues (Oct, MOFO, DIFO, DIBO, DIBAC, BARAC) and their rate constants (in $M^{-1} s^{-1}$) for reactions with benzyl azide. (b) Cycloaddition reactions of BARAC analogues **1–11** with benzyl azide.

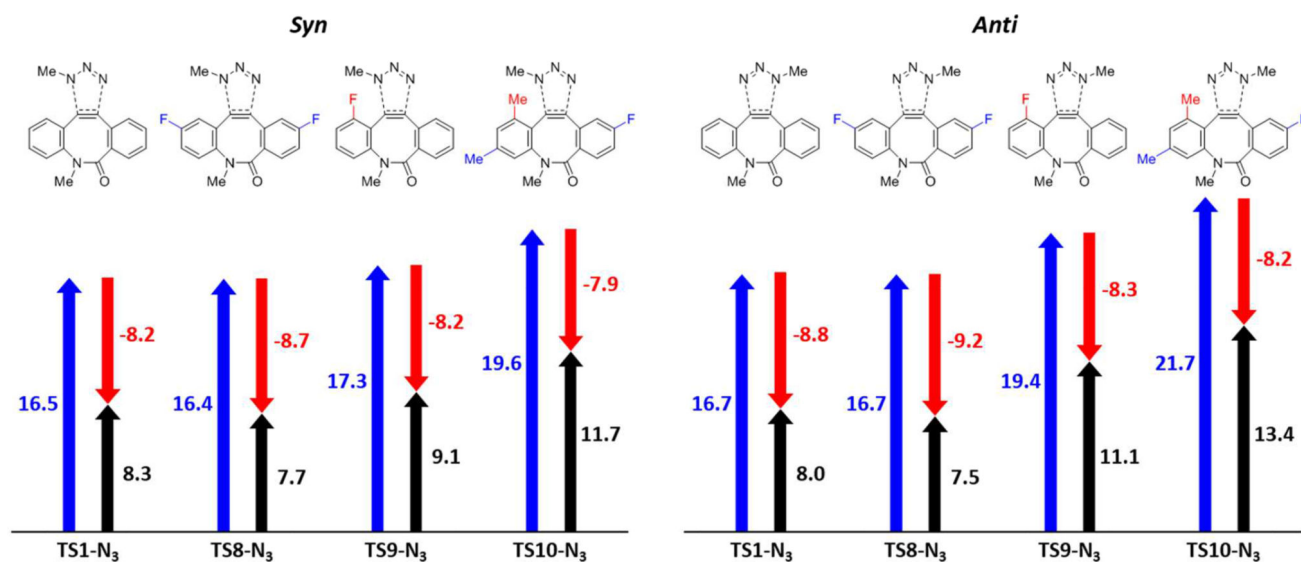


Figure 8.
D/I analysis of reactions of methyl azide with BARAC analogues **1** and **8–10**.

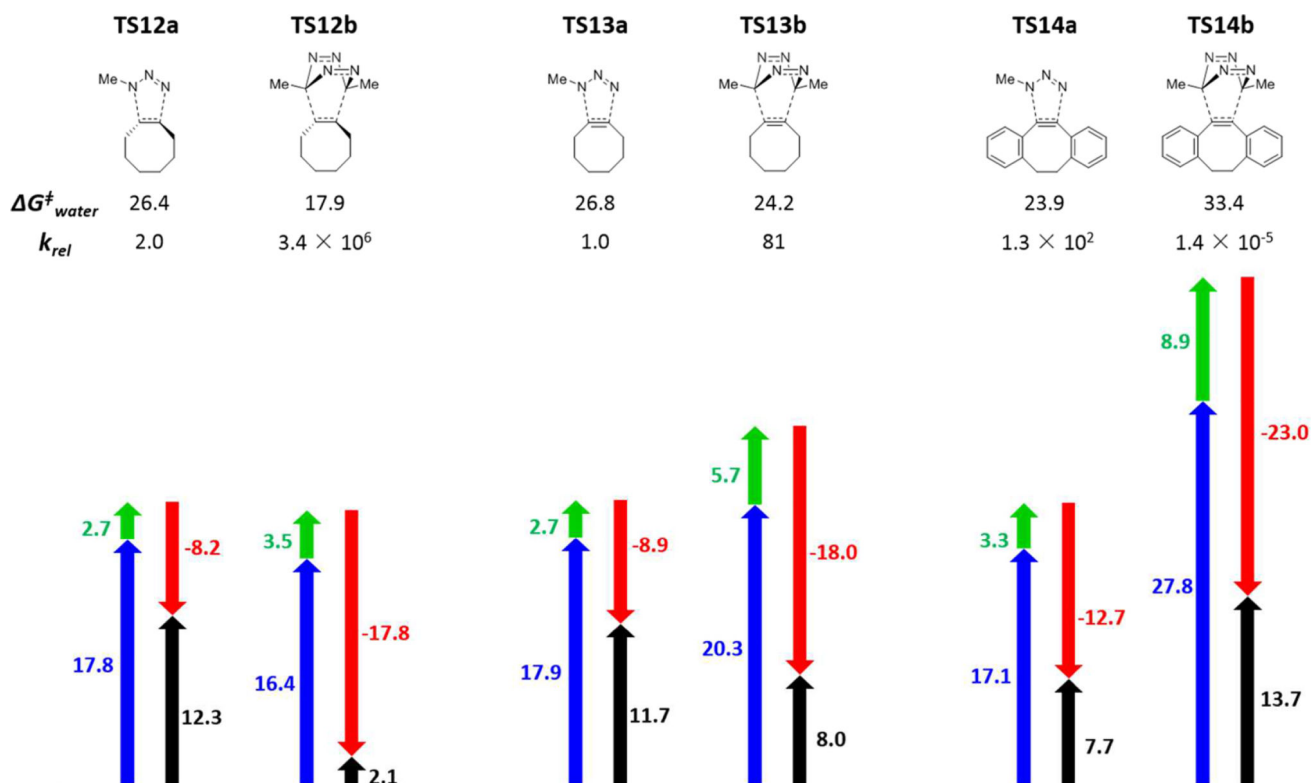


Figure 9.
D/I analyses of reactions of methyl azide and dimethyltetrazine with *trans*-cyclooctene, cyclooctyne, and dibenzocyclooctyne. Calculated energies are shown in kcal/mol.

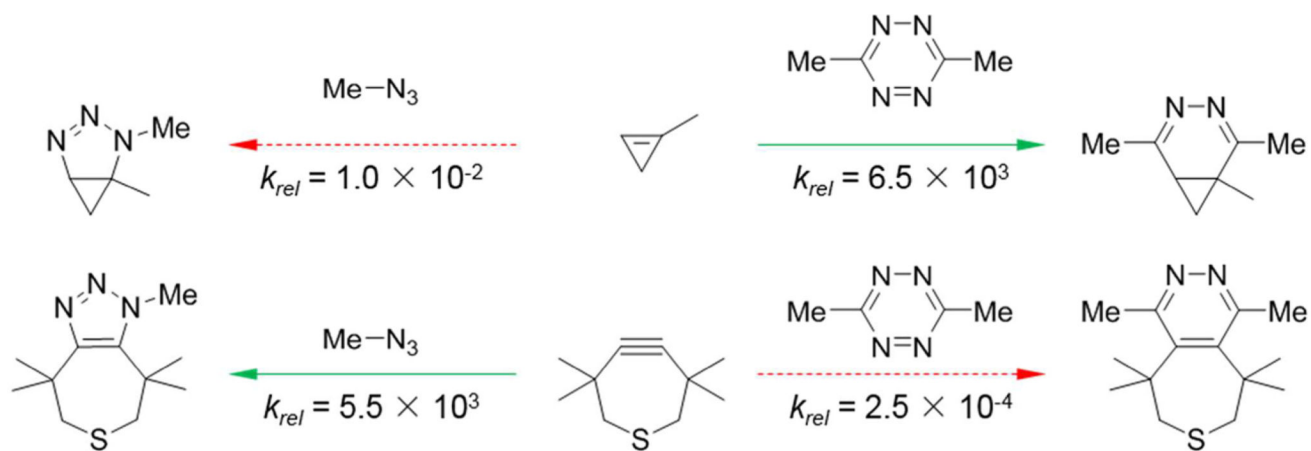


Figure 10.
Computationally designed mutually orthogonal cycloadditions.

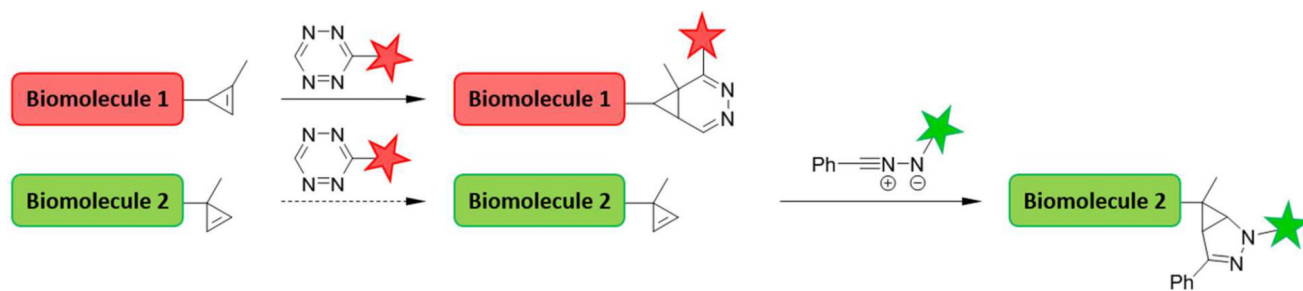


Figure 11. Orthogonal reactions of 1,3-disubstituted cyclopropenes with tetrazines and 3,3-disubstituted cyclopropenes with nitrile imines.

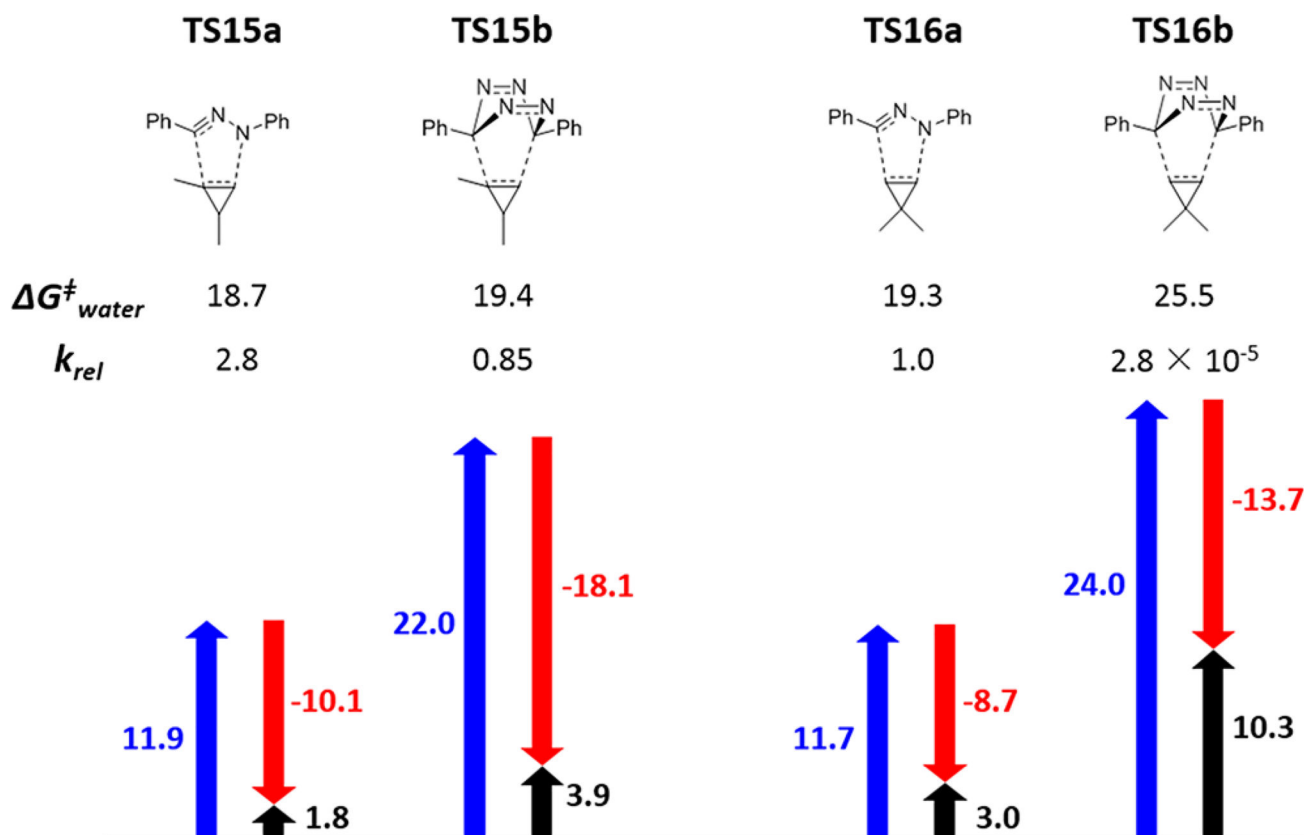


Figure 12.

D/I analysis of reactions of nitrile imine and tetrazine with 1,3- and 3,3-dimethylcyclopropene. Calculated energies are shown in kcal/mol.

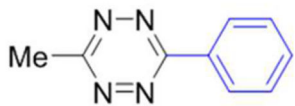
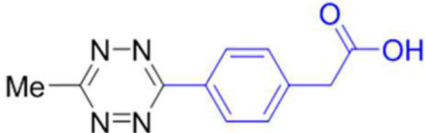
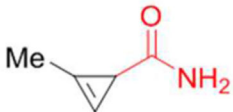
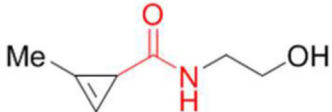





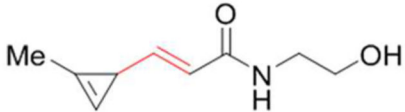
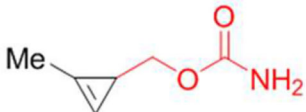
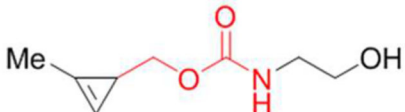

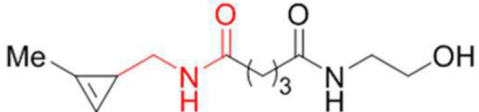
 $k_{\text{compt}} (\text{M}^{-1} \text{s}^{-1})$	 $k_{\text{expt}} (\text{M}^{-1} \text{s}^{-1})$
 0.0045	 0.0047
 0.067	 0.74
 1.0	 0.336
 2.3	 0.20
 0.13	 0.366
 0.16	 0.65

Figure 13.

Tetrazine ligation with 1-methyl-3-substituted cyclopropenes: (left) computed rate constants (k_{compt}); (right) experimentally measured rate constants (k_{expt}). The substrates used in the calculations were simplified versions of those used in the experiments.

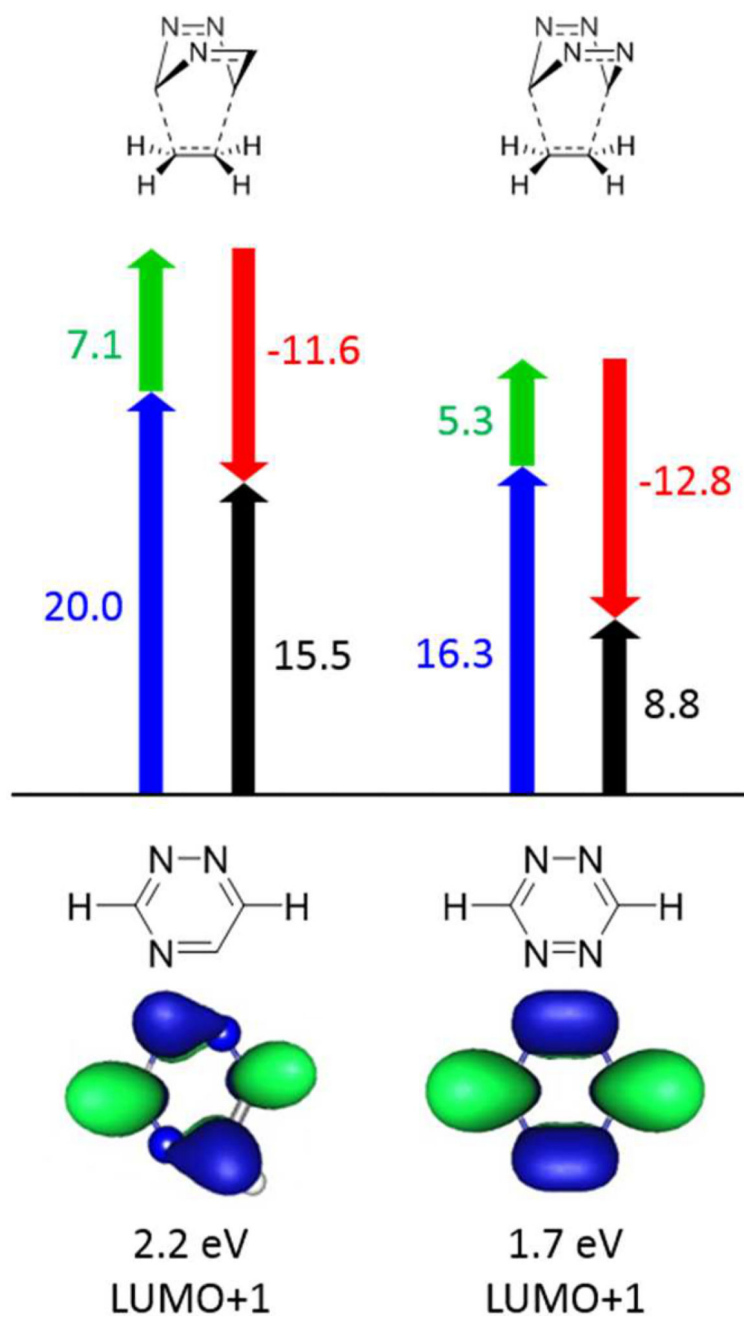


Figure 14. D/I analysis of the reactions of 1,2,4-triazine and 1,2,4,5-tetrazine with ethylene and the LUMO+1 energies of 1,2,4-triazine and 1,2,4,5-tetrazine.

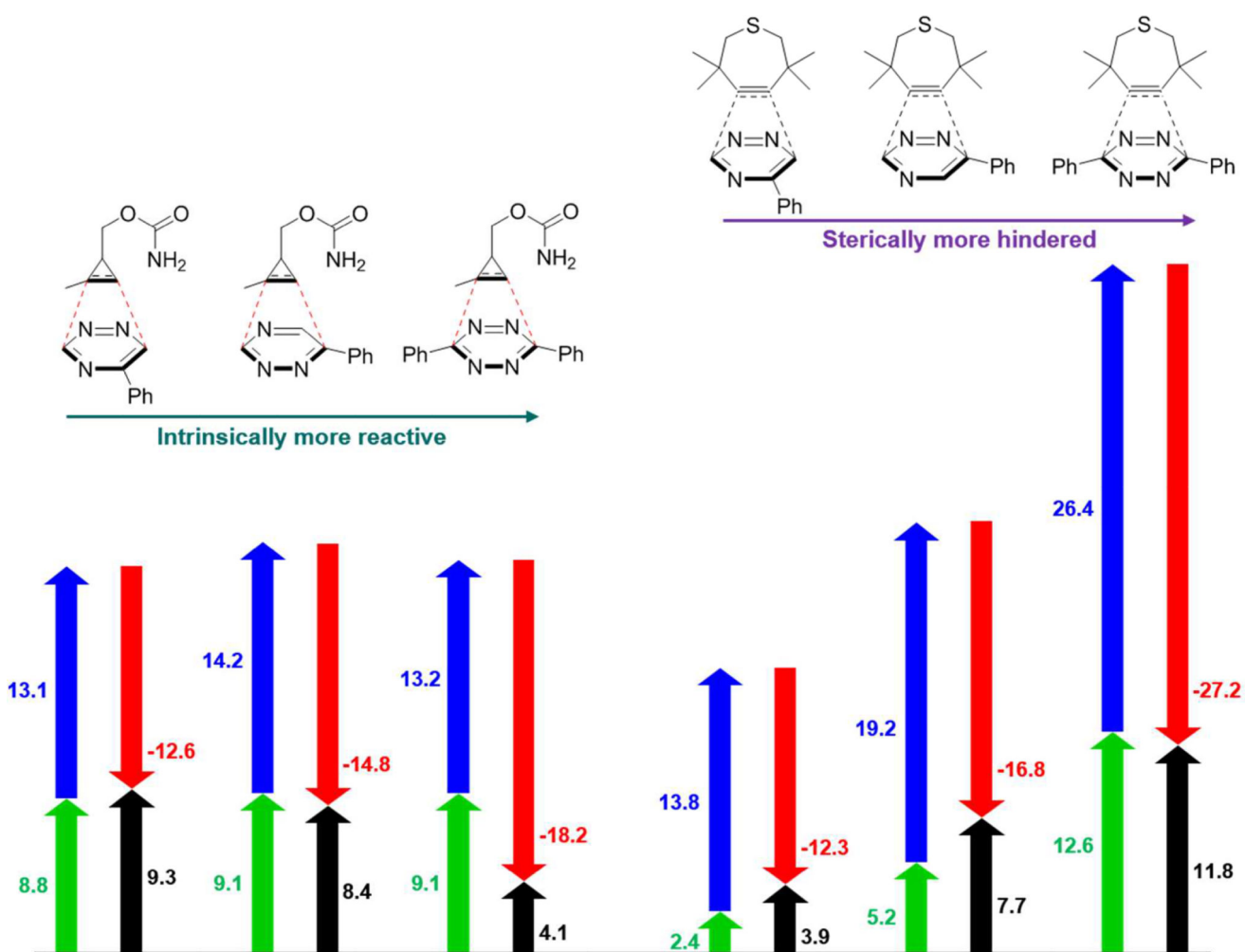


Figure 15.
D/I analysis of factors controlling mutually orthogonal cycloadditions involving triazines and tetrazines.

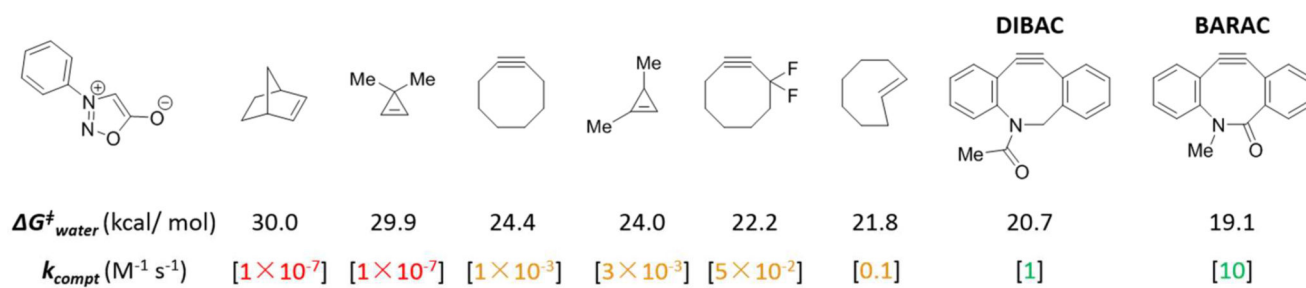


Figure 16. Computational screening of cycloadditions of *N*-phenylsydnone (3 + 2) with dipolarophile candidates.

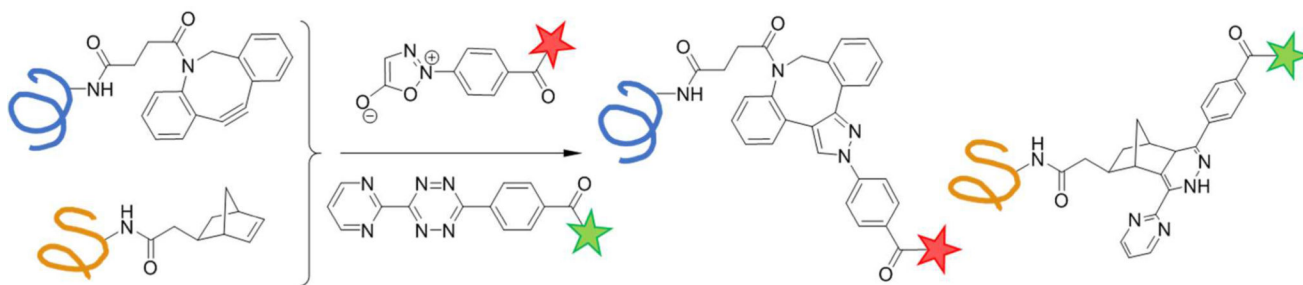


Figure 17.
Mutual orthogonal cycloadditions of sydnone and tetrazine.

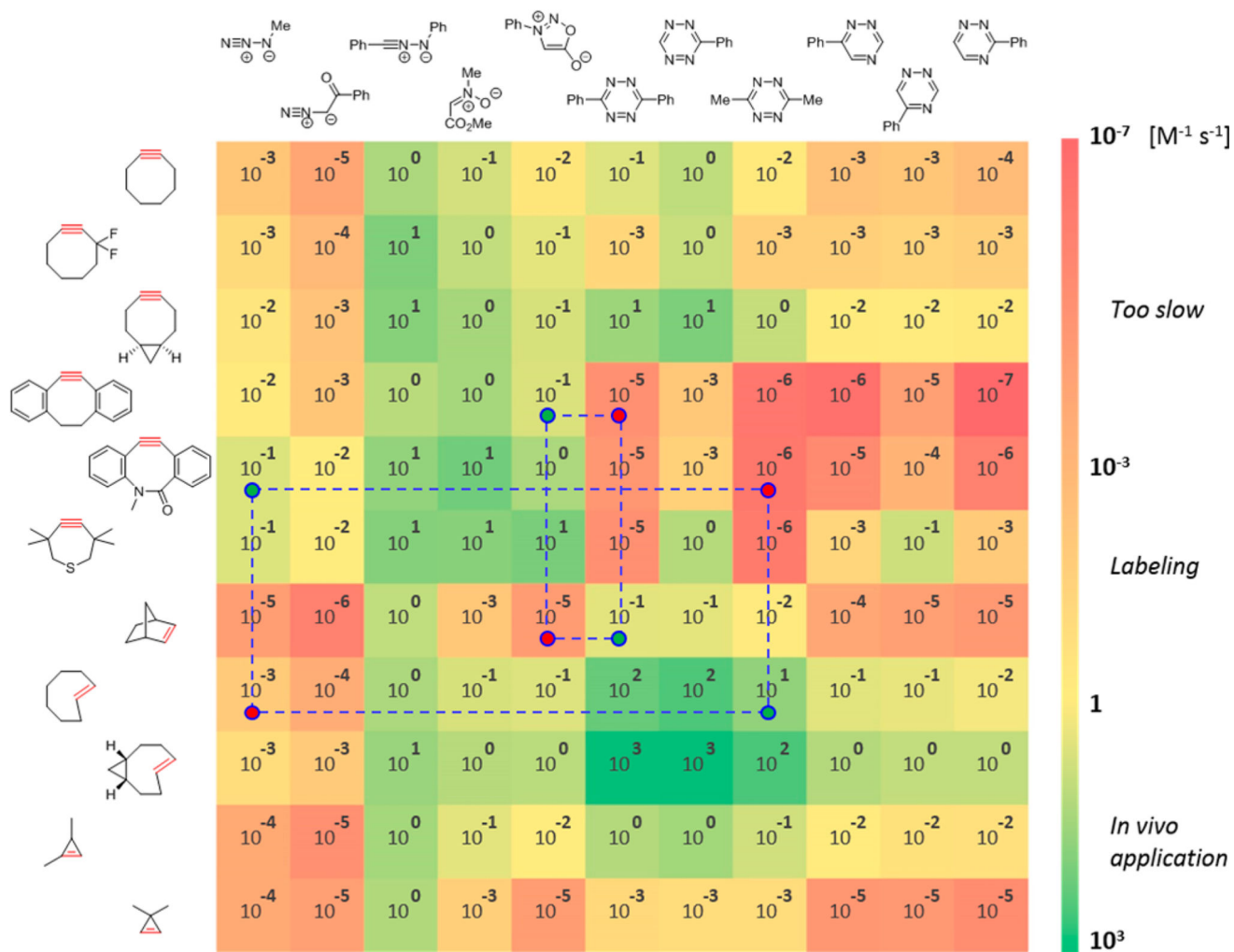


Figure 18.

Reactivity matrix of cycloaddition reactions among known bioorthogonal compounds. Each box is color-coded according to the calculated second-order rate constant. Mutual orthogonal cycloaddition pairs are shown on the corners of the dashed boxes: green circles represent rapid reactions, while red circles stand for slow/unlikely reactions.